Few-Body Systems 0, 1–11 (2000)

Few-Body Systems



# Study of the $^3$He($^4$He, $\gamma$)$^7$Be and $^3$H($^4$He, $\gamma$)$^7$Li Reactions in an Extended Two-Cluster Model*

Attila Csótó[1], Karlheinz Langanke[2]

[1] Department of Atomic Physics, Eötvös University, Pázmány Péter sétány 1/A, H–1117 Budapest, Hungary

[2] Institute for Physics and Astronomy, Aarhus University, DK-8000 Aarhus, Denmark

**Abstract.** The $^3$He($^4$He, $\gamma$)$^7$Be and $^3$H($^4$He, $\gamma$)$^7$Li reactions are studied in an extended two-cluster model which contains $\alpha + h/t$ and $^6$Li $+ p/n$ clusterizations. We show that the inclusion of the $^6$Li $+ p/n$ channels can significantly change the zero-energy reaction cross sections, $S(0)$, and other properties of the $^7$Be and $^7$Li nuclei, like the quadrupole moments $Q$. However, the results agree with the known correlation trend between $S(0)$ and $Q$. Moreover, we demonstrate that the value of the zero-energy derivatives of the astrophysical S-factors are more uncertain than currently believed.

## 1 Introduction

The $^3$H($^4$He, $\gamma$)$^7$Li and $^3$He($^4$He, $\gamma$)$^7$Be reactions play important roles in astrophysics. The former process is an important ingredient in big-bang nucleosynthesis, while the latter one is a key reaction in the solar p-p (proton-proton) chains. The $^3$He($^4$He, $\gamma$)$^7$Be reaction produces $^7$Be in our Sun, which is destroyed by either the capture of an electron or a proton in the $^7$Be($p, \gamma$)$^8$B process. In both cases, neutrinos are generated which are observable by terrestrial detectors and thus contribute to the solar neutrino problems [1]. The production rate of $^7$Be in the Sun is determined by the competition of the $^3$He($^4$He, $\gamma$)$^7$Be and $^3$He($^3$He, $2p$)$^4$He reactions. Therefore, the precise knowledge of these cross sections at the most effective solar energies ($\approx 20$ keV) is an important input to solar models and to the possible solution of the solar neutrino problems.

There exist several measurements on the $^3$He($^4$He, $\gamma$)$^7$Be cross section down to energies of about 100 keV. From these data, the reaction rate at solar energies is obtained by extrapolation. The $^3$He + $^4$He fusion reaction at low energies is usually viewed as an approximate external capture process [2]. Thus,

*Dedicated to Achim Weiguny on the occasion of his 65th birthday the energy dependence of the cross section can then be obtained from a simple $^3$He+$^4$He potential model, which in fact reproduces the energy dependence of the measured data rather well. The most recent compilation of the data quotes the $^3$He($^4$He, $\gamma$)$^7$Be cross section as $S_{34}(0) = 0.53 \pm 0.05$ keVb [3], where the rather small uncertainty mainly reflects differences in the absolute normalization of the cross section. As customary, we have used the standard S-factor parametrization of the cross section (the subscript '34' stands for $^3$He + $^4$He)

$$S(E) = \sigma(E) E \exp\left[2\pi\eta(E)\right], \qquad \eta(E) = \frac{\mu Z_1 Z_2 e^2}{k\hbar^2}, \tag{1}$$

where $Z_1$ and $Z_2$ are the charge numbers of the fragments in the incoming channel, while $\mu$ and $k$ are their reduced mass and wave number, respectively.

There exist also more elaborate theoretical studies of the $^3$H($^4$He, $\gamma$)$^7$Li and $^3$He($^4$He, $\gamma$)$^7$Be reactions in the literature, which are based on the resonating group method or the related microscopic potential model [4, 5, 6, 7, 8, 9, 10]. These microscopic studies, based on a single $^3$He + $^4$He fragmentation, yield an energy dependence of the $^3$He($^4$He, $\gamma$)$^7$Be cross section, which is similar to the potential models. Furthermore as a success of these approaches, they correctly predicted [7, 5] the low-energy $^3$H($^4$He, $\gamma$)$^7$Li cross section in absolute normalization and energy dependence, which has been subsequently confirmed by the precision measurement of Brune *et al.* [11].

Why do we then want to study these low-energy reactions again? Despite its apparently successful agreement with data, the dependence of the cross section on the enlargement of the model space has not been yet established. A first attempt has been made by Mertelmeier and Hofmann [6] who included additionally a $^6$Li + $p$ configuration in their model space. This multichannel RGM calculation shows a somewhat increased S-factor compared to the single-channel case, while the rise towards lower energies is reduced. Given the astrophysical relevance it is important to determine whether this weaker energy dependence is physical or an artifact caused by the approximate treatment of the asymptotic Whittaker functions in the bound states. Second, we have found in Ref. [12] that taking into account the $^6$Li + $p$ clusterization changes some of the key properties of the $^7$Be bound states considerably. For example, the $^7$Be quadrupole moment is increased by about $0.5 - 1.0$ $e$fm$^2$ if the $^6$Li + $p$ configuration is added to the dominant $^3$He + $^4$He clusterization.

In the present work we study the $^3$He($^4$He, $\gamma$)$^7$Be and $^3$H($^4$He, $\gamma$)$^7$Li reactions in an extended two-cluster model, which can take into account the $^6$Li + $p/n$ clusterization, in addition to the more important $^4$He + $^3$He/$^3$H configurations. Our main goal is to explore how much the energy dependence of the low-energy $^3$He($^4$He, $\gamma$)$^7$Be cross section is affected by the addition of the $^6$Li + $p$ configuration. The simultaneous study of the $^3$H($^4$He, $\gamma$)$^7$Li reaction serves as a potential check, as in this case the low-energy cross section is known rather well.

## 2 Model

Our study of the $^3\mathrm{He}(^4\mathrm{He},\gamma)^7\mathrm{Be}$ and $^3\mathrm{H}(^4\mathrm{He},\gamma)^7\mathrm{Li}$ reactions is based on the microscopic cluster model. As a model space we adopt the dominant $^4\mathrm{He}+{}^3\mathrm{He}/^3\mathrm{H}$ clusterization, to which the $^6\mathrm{Li}+p/n$ configuration is added as well. For comparison, we also perform calculations based solely on the $^4\mathrm{He}+{}^3\mathrm{He}/^3\mathrm{H}$ clusterization; in this case our studies correspond to the microscopic calculations presented in [4, 5, 6, 7, 8, 9, 10]. Our wave functions thus have the general form

$$\Psi^{J^\pi}_{^7\mathrm{Be}} = \mathcal{A}\left\{\left[\left[\Phi^\alpha\Phi^h\right]_{1/2}\chi_L(\boldsymbol{\rho}_1)\right]_{JM}\right\} + \sum_{L,S}\mathcal{A}\left\{\left[\left[\Phi^{^6\mathrm{Li}}\Phi^p\right]_S\chi_L(\boldsymbol{\rho}_2)\right]_{JM}\right\} \tag{2}$$

and

$$\Psi^{J^\pi}_{^7\mathrm{Li}} = \mathcal{A}\left\{\left[\left[\Phi^\alpha\Phi^t\right]_{1/2}\chi_L(\boldsymbol{\rho}_1)\right]_{JM}\right\} + \sum_{L,S}\mathcal{A}\left\{\left[\left[\Phi^{^6\mathrm{Li}}\Phi^n\right]_S\chi_L(\boldsymbol{\rho}_2)\right]_{JM}\right\}. \tag{3}$$

Here $\mathcal{A}$ is the intercluster antisymmetrizer, the internal cluster states $\Phi$ are translationally invariant harmonic oscillator shell model states ($\alpha = {}^4\mathrm{He}$, $h = {}^3\mathrm{He}$, and $t = {}^3\mathrm{H}$), the $\boldsymbol{\rho}$ vectors are the various intercluster Jacobi coordinates, $L$ and $S$ are the total orbital angular momentum and spin, respectively, $J$ is the total angular momentum, and [...] denotes angular momentum coupling. The spin-parity of the $^6\mathrm{Li}$ ground state is $1^+$, and the total parity is $\pi = (-1)^L$. Using (2) or (3) in the seven-nucleon Schrödinger equation, we arrive at an equation for the intercluster relative motion functions $\chi$. These equations must be solved with high precision up to large $\rho$ value, because the electromagnetic transition strengths are shifted towards large $\rho$ at the low solar energies. For the $\alpha + h/t$ scattering we neglect the $^6\mathrm{Li}$ channels and solve the relative-motion equations by using the variational Kohn-Hulthén method [13]. For the bound states we use a version of the so-called Siegert variational method, which was first applied in cluster model calculations by Fiebig and Weiguny [14]. In this method the relative motions $\chi$ are expanded in terms of square integrable functions (Gaussians in our case) plus a term with the correct asymptotics.

We study only E1 transitions here. After setting up the initial scattering wave functions and final bound states, the E1 cross section is calculated [6, 15] as

$$\sigma(E) = \sum_{J_i,J_f}\frac{1}{2}\frac{16\pi}{9\hbar}\left(\frac{E_\gamma}{\hbar c}\right)^3\sum_{L_\omega}(2L_\omega+1)^{-1}|\langle\Psi^{J_f}||\mathcal{M}^E_1||\Psi^{J_i}_{L_\omega}\rangle|^2, \tag{4}$$

where $\mathcal{M}^E_1$ is the electric dipole ($E1$) transition operator, $\omega$ represents the entrance channel, $E_\gamma$ is the photon energy, and $J_f$ and $J_i$ are the total spin of the final and initial state, respectively. The initial wave function $\Psi^{J_i}_{L_\omega}$ is a partial wave of a unit-flux scattering wave function.

## 3 Results

Meaningful cluster calculations of the $^3\mathrm{He}(^4\mathrm{He},\gamma)^7\mathrm{Be}$ and $^3\mathrm{H}(^4\mathrm{He},\gamma)^7\mathrm{Li}$ reactions within our chosen model space of $\alpha + h/t$ and $^6\mathrm{Li} + p/n$ configurations should satisfy the following conditions: (i) the experimental value of the $^7$Be/$^7$Li ground state energy with respect to the $\alpha + h/t$ threshold must be reproduced; (ii) the experimental value of the spin-orbit splitting between the $3/2^-$ and $1/2^-$ states in $^7$Be/$^7$Li has to be correct; (iii) in the extended model spaces the $^6$Li $+ p/n$ threshold must be at the right position, relative to $\alpha + h/t$. Besides calculations for the extended model space $\{\alpha + h/t; {}^6\mathrm{Li} + p/n\}$, we also perform studies in the single-channel $\alpha + h/t$ model space, corresponding to the previous calculations (e.g. [7, 9]). In the later case only constraints (i) and (ii) have been fulfilled by adjustments of the NN interaction.

The internal structure of the $^6$Li cluster is described in our model as an $\alpha + d$ clusterization with an $s$-wave deuteron and $l = 0$ relative motion between the $\alpha$ and $d$ clusters. Varying the size parameters of the $\alpha$ and $d$ clusters inside $^6$Li should allow us to satisfy condition (iii), while the other two conditions can be met by fine-tuning the effective nucleon-nucleon interaction. In our previous multicluster study of the $^7$Be$(p, \gamma)^8$B reaction, the Minnesota (MN) force [16] has been identified as the most reliable interaction. Therefore we will also use it in the present calculation, even at the expense that it slightly overestimates the total cross sections for both reactions studied here. In the MN interaction, the exchange mixture parameter ($u$) and spin-orbit strength are those parameters that are slightly varied. Additionally, we perform calculations with the MHN interaction [17] which, as shown by Kajino, reproduces the measured cross section data for both reactions in a single-channel $\alpha + h/t$ model quite well.

Choosing the cluster size parameter $\beta = 0.4$ fm$^{-2}$ and by fine-tuning the MN interaction we have exactly reproduced the binding energies of the two bound states in $^7$Be and $^7$Li with respect to the $\alpha$+h/t threshold. This leads to $u = 1.049$ and $V_{\mathrm{SO}} = -27.85$ MeV, $u = 1.044$ and $V_{\mathrm{SO}} = -26.7$ MeV, $u = 1.008$ and $V_{\mathrm{SO}} = -35.94$ MeV, and $u = 0.998$ and $V_{\mathrm{SO}} = -36.8$ MeV, respectively for the exchange mixture parameter of the central force and the strength of the spin-orbit force in the cases of one-channel $^7$Li, two-channel $^7$Li, one-channel $^7$Be, and two-channel $^7$Be, respectively. For the $^6$Li binding energy we calculate 1.43 MeV, to be compared with the experimental value of 1.475 MeV [18]. In the case of the MHN interaction, by choosing $\beta = 0.56$ fm$^{-2}$ and fine-tuning the $m$ parameter in the Gaussian of medium-size range (the sum of the Wigner and Majorana parameters is kept fixed at the original MHN value), we reproduce the binding energies in $^7$Be and $^7$Li, while, however, the $^6$Li $+ p/n$ threshold energy is overestimated by about 1.5 MeV, relative to $\alpha + h/t$; i.e. condition (iii) cannot be satisfied. The corresponding potential parameters, following the same order as above, are $m = 0.399$ and $V_{\mathrm{SO}} = -854.6$ MeV, $m = 0.444$ and $V_{\mathrm{SO}} = -1393$ MeV, $m = 0.399$ and $V_{\mathrm{SO}} = -840.4$ MeV, and $m = 0.450$ and $V_{\mathrm{SO}} = -1450$ MeV, respectively, where $V_{\mathrm{SO}}$ is the strength of the long-range spin-orbit force.

In the partial waves which contribute significantly to the capture cross sections, our interactions give generally more repulsive higher-energy phase shifts than those indicated by phenomenological analyses. As an example, we show our $^4$He + $^3$He phase shifts in Fig. 1. It is particularly noteworthy that the phase shifts are more repulsive in the two-channel calculations than in the one-channel case. This is related to the fact that the point-nucleon matter radius of the com-

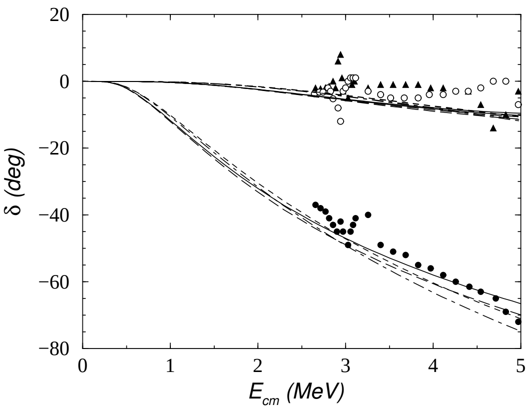


**Figure 1.** $^4$He + $^3$He scattering phase shifts in the $J^\pi = 1/2^+$ (filled circle), $3/2^+$ (filled triangle), and $5/2^+$ (open circle) partial waves. The solid (short-dashed) and long-dashed (dot-dashed) curves show the results obtained with the MN (MHN) interaction for the $\alpha + h$ and $\{\alpha + h; ^6\mathrm{Li} + p\}$ model spaces, respectively. The calculated phase shifts in the $3/2^+$ and $5/2^+$ partial waves nearly coincide. The data are taken from [19].

bined nucleus increases by the enlargement of the model space (see Tables 1 and 2 below).

The S-factors, calculated for the extended and single-channel model spaces and both interactions, are compared to the data in Fig. 2. As mentioned above, in the single-channel case the MN interaction overestimates the low-energy $^3\mathrm{He}(^4\mathrm{He},\gamma)^7\mathrm{Be}$ and $^3\mathrm{H}(^4\mathrm{He},\gamma)^7\mathrm{Li}$ reactions, while the MHN force agrees with the data quite well. However, more importantly for the present study, the extended model space yields noticeably larger S-factors than in the single-channel model (the reason for this increase will be discussed below) for both interactions. But we also note that the slope of the low-energy S-factor changes slightly when comparing the results for the two model spaces. This finding can be quantified by the value of $S^{-1}dS/dE\,(0)$ which decreases from $-0.53$ ($-0.56$) MeV$^{-1}$ to $-0.56$ ($-0.63$) MeV$^{-1}$ for the MN (MHN) interaction in the case of the $^3$He+$^4$He fusion reaction, if we add the $^6\mathrm{Li} + p$ configuration. This result is our first indication that the reaction cannot be treated as a totally external process. As a consequence, the usual strategy to adopt the energy dependence of a potential model S-factor and normalize it to the measured data becomes slightly questionable as it explicitly assumes that the model differs from the data only by the asymptotic normalization constant.

In order to explore the origin of the cross section changes between the extended and single-channel model spaces, we employ a strategy already applied in [7] and, for the $^7\mathrm{Be}(p,\gamma)^8\mathrm{B}$ reaction, in [12]. Using the MN interaction for this exploration we repeat the calculations for different cluster size parameters ($\beta = 0.48$ and $0.56$ fm$^{-2}$) and try to observe correlations between $S(0)$ and other observables in $^7$Be and $^7$Li, respectively. The calculations have been performed again in both the single-channel $\alpha + h/t$ and the extended $\{\alpha + h/t; ^6\mathrm{Li} + p/n\}$ model space. While the above conditions (i)−(iii) could be fulfilled in each study by a suited adjustment of the interaction, the $^6$Li ground state energy is now

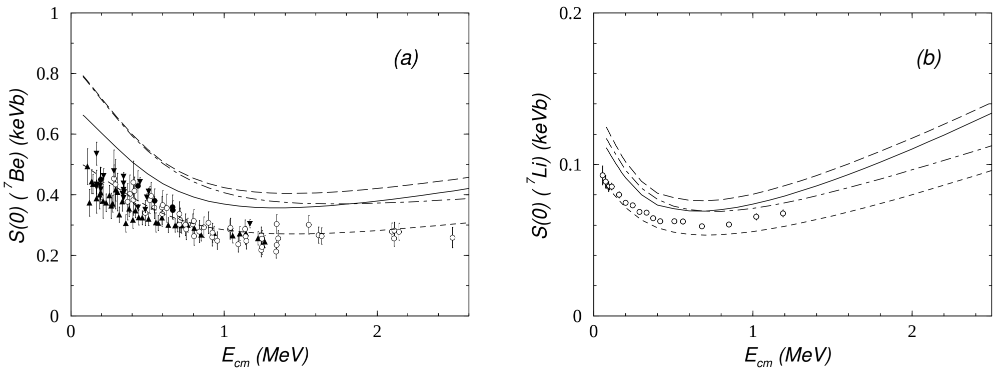


**Figure 2.** Comparison of the calculated astrophysical S-factor $S(E)$ of the $^3$He($^4$He, $\gamma$)$^7$Be (a) and $^3$H($^4$He, $\gamma$)$^7$Li (b) reactions with data. The solid (short-dashed) and long-dashed (dot-dashed) curves show the results obtained with the MN (MHN) interaction for the $\alpha + h/t$ and $\{\alpha + h/t; ^6\mathrm{Li} + p/n\}$ model spaces, respectively. The $^7$Be and $^7$Li experimental data are taken from [20] and [11], respectively (the symbols follow the notation of Ref. [3]).

underbound relative to the $\alpha + d$ threshold; we find $-1.12$ MeV and $-0.39$ MeV for $\beta = 0.48$ and $0.56$ fm$^{-2}$, respectively. As a consequence of this underbinding, the $\alpha + d$ separation in the $^6$Li ground state is too large. At the same time, the radius of the $\alpha$ particle inside $^6$Li gets smaller, if $\beta$ is increased from 0.4 fm$^{-2}$ to 0.56 fm$^{-2}$. These too effects together will render the results obtained for $\beta = 0.48$ fm$^{-2}$ and 0.56 fm$^{-2}$ rather unphysical, but might still allow to draw conclusions about the correlations of the cross section with other $^7$Be and $^7$Li properties.

In Fig. 3 we demonstrate the effect of the cluster size parameter on the elastic phase shifts, exemplified for the two-channel study of the $^3$He+$^4$He reaction. We observe that the phase shifts get increasingly more attractive if the width parameter $\beta$ increases. This is related to the fact that, with increasing $\beta$, the

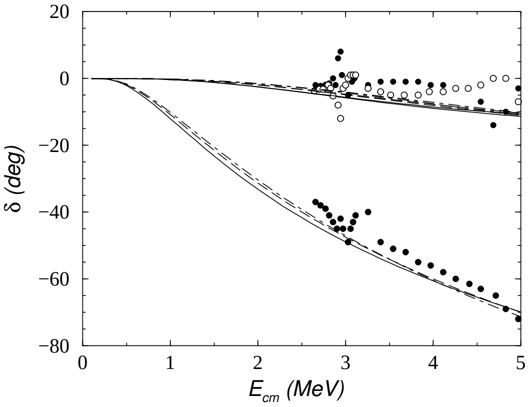


**Figure 3.** $^4$He+$^3$He scattering phase shifts in the $J^\pi = 1/2^+$ (filled circle), $3/2^+$ (filled triangle), and $5/2^+$ (open circle) partial waves. The calculations have been performed in the $\{\alpha + h; ^6\mathrm{Li} + p\}$ model space with the MN interaction and various cluster size parameters, $\beta = 0.4$ fm$^{-2}$ (solid curves), $\beta = 0.48$ fm$^{-2}$ (long-dashed curves), and $\beta = 0.56$ fm$^{-2}$ (dot-dashed curves). The data are taken from [19].

**Table 1.** Calculated quadrupole moments ($Q$) and point-nucleon matter rms radii ($r$) of $^7$Be, and the zero-energy astrophysical S-factor [$S(0)$] and its derivative [$S^{-1}dS/dE\,(0)$] of the $^3$He($^4$He, $\gamma$)$^7$Be reaction in the various model spaces. The entries denoted by * are for the MHN interaction, while the rest is for the MN force.

| Model ($\beta$) | $S(0)$ (keVb) | $S^{-1}dS/dE\,(0)$ (MeV$^{-1}$) | $Q$ ($e$fm$^2$) | $r$ (fm) |
|---|---|---|---|---|
| $\{\alpha+h;{}^6\text{Li}+p\}$ | | | | |
| 0.4 | 0.83 | −0.57 | −7.23 | 2.62 |
| 0.48 | 0.91 | −0.61 | −7.28 | 2.56 |
| 0.56 | 1.16 | −0.70 | −7.41 | 2.54 |
| 0.56* | 0.83 | −0.64 | −6.64 | 2.43 |
| $\alpha+h$ | | | | |
| 0.4 | 0.70 | −0.53 | −6.61 | 2.55 |
| 0.48 | 0.64 | −0.51 | −6.40 | 2.44 |
| 0.56 | 0.59 | −0.50 | −6.22 | 2.36 |
| 0.56* | 0.52 | −0.52 | −6.27 | 2.51 |

sizes of the combined nuclei $^7$Li and $^7$Be shrink (see Tables 1 and 2). Without explicitly showing it in a figure, we note that the dependence of the phase shifts on the cluster size parameter is slightly stronger in the one-channel case.

Tables 1 and 2 list our results for the zero-energy cross sections, $S(0)$, and the quadrupole moments and point-nucleon matter rms radii of $^7$Be and $^7$Li. The $S(0)$ values were determined from fits to the calculated S-factors in the $E = 0.1 - 0.9$ MeV interval, using the formula given in Ref. [8],

$$S(E) = S(0)\exp(-\alpha E)\Big(1 + a_2E^2 + a_3E^3 + a_4E^4\Big). \qquad (5)$$

As shown in Fig. 4, $S(0)$ and the quadrupole moment $Q$ of $^7$Be/$^7$Li are nicely

**Table 2.** The same as Table 1, except for $^7$Li and the $^3$H($^4$He, $\gamma$)$^7$Li reaction.

| Model ($\beta$) | $S(0)$ (keVb) | $S^{-1}dS/dE\,(0)$ (MeV$^{-1}$) | $Q$ ($e$fm$^2$) | $r$ (fm) |
|---|---|---|---|---|
| $\{\alpha+t;{}^6\text{Li}+n\}$ | | | | |
| 0.4 | 0.148 | −2.26 | −3.83 | 2.55 |
| 0.48 | 0.156 | −2.11 | −3.78 | 2.48 |
| 0.56 | 0.184 | −2.07 | −3.80 | 2.46 |
| 0.56* | 0.138 | −2.10 | −3.51 | 2.36 |
| $\alpha+t$ | | | | |
| 0.4 | 0.131 | −2.19 | −3.77 | 2.50 |
| 0.48 | 0.122 | −1.98 | −3.75 | 2.39 |
| 0.56 | 0.117 | −1.82 | −3.73 | 2.31 |
| 0.56* | 0.099 | −1.96 | −3.52 | 2.28 |

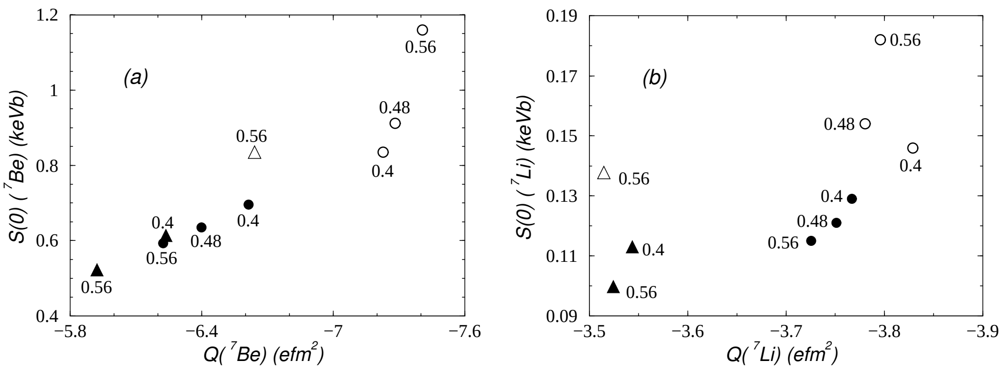


**Figure 4.** The zero-energy astrophysical S-factors of the $^3$He($^4$He, $\gamma$)$^7$Be (a) and $^3$H($^4$He, $\gamma$)$^7$Li (b) reactions as a function of the quadrupole moment of $^7$Be and $^7$Li, respectively. The filled and open circles show the results for the MN interaction coming from the $\alpha + h/t$ and $\{\alpha + h/t; {}^6\text{Li} + p/n\}$ model spaces, respectively. The triangles denote the analogous quantities in the case of the MHN force. The values of the harmonic oscillator size parameter ($\beta$) are indicated.

correlated in the single-channel $\alpha + h/t$ models. Although the results of the $\{\alpha + h/t; {}^6\text{Li} + p/n\}$ model space with $\beta = 0.4$ fm$^{-2}$ fit well into the trend, the results for $\beta = 0.48$ and $0.56$ fm$^{-2}$ do not. We believe that in the case of $^7$Be this is due to the disappearing $\alpha + d$ binding energy inside $^6$Li, while for $^7$Li, it is caused by the adverse behavior of the $\alpha$ and $^6$Li sizes.

The correlation between $S(0)$ and $Q$, shown in Fig. 4, can easily be understood by recalling that for external capture reactions, at energies deep below the Coulomb barrier, the $S(0)$ cross section is practically fully determined by the asymptotic normalization constants of the bound state wave functions; the $^7$Be($p, \gamma$)$^8$B is a well-known example [12]. These normalization constants in turn are sensitive mainly to the radii of the effective $\alpha - h/t$ potentials. While going from $\beta = 0.56$ to $0.4$ fm$^{-2}$ in the $\alpha + h/t$ model, the sizes of the clusters (and thus the radii of the $\alpha - h/t$ potentials) increase, which explains the increase in $S(0)$ and $Q$. When the $^6$Li$ + p/n$ channel is added, $S(0)$ is further increased. Note that $^6$Li is bigger than $^7$Be/$^7$Li. Thus the radii of the $\alpha - h/t$ potentials are effectively increased by adding the $^6$Li $+ p/n$ component.

As we have already pointed out in Ref. [12], the $^6$Li $+ p$ channel has a substantial effect on the quadrupole moment of $^7$Be. As one can see in Fig. 4(a), the inclusion of the $^6$Li channel in the $\beta = 0.4$ fm$^{-2}$ model results in a roughly 10% increase in $Q$. At the same time, the extension of the $^7$Li model space leads to just a 1.6% increase in the quadrupole moment of that nucleus. The explanation of this phenomenon is natural: the $^6$Li $+ p$ configuration brings in a large charge polarization, which strongly affects the quadrupole moment of $^7$Be, while there is no such effect for $^7$Li.

In Ref. [7] Kajino suggested to determine the zero-energy $^3$He($^4$He, $\gamma$)$^7$Be astrophysical S-factor indirectly from the correlations between $S_{34}(0)$ and the quadrupole moment of $^7$Li. This proposal, however, is spoiled if the $^7$Li quadrupole moment is indeed as large as $-4.0$ $e$fm$^2$, as currently favored [18, 21], and thus noticeably different than the value of $-(3.4 - 3.7)$ $e$fm$^2$ [22], accepted at the time Kajino performed his analysis. From Fig. 4 we observe that the large $Q$-value corresponds to a cross section $S(0) \approx 0.19$ keVb for the $^3\mathrm{H}(^4\mathrm{He},\gamma)^7\mathrm{Li}$ reaction, which is about twice the value derived from the precision data of [11]. This apparent shortcoming might point to the necessity to explicitly consider the interference with the internal $^6$Li quadrupole moment in cluster studies.

As we mentioned, our $S(0)$ values were determined by fitting the calculated $S(E)$ functions by a polynomial form between 0.1 and 0.9 MeV. Additionally, Tables 1 and 2 list the results for $S^{-1}dS/dE\,(0)$. In addition to this fit, we tested another functional form for the low-energy S-factors, suggested in Ref. [23]. The

$$S(E) = n\frac{1 + c_1E + c_2E^2}{E + E_B} \tag{6}$$

expression reflects the fact that S has a pole at the binding energy $E_B$ of $^7$Be/$^7$Li, relative to the $\alpha + h/t$ threshold. In order to get good fits even at rather low energies, we needed to use higher-order terms in the numerator of Eq. (6). This shows the importance of the non-asymptotic contributions to the cross sections. With a fourth-order polynomial in the numerator in Eq. (6), we get practically the same results as shown in Table 1. One might conclude from our results that the $S'_{34}(0)$ values, as determined in Ref. [3] or in Ref. [7] (for both the $^7$Be and $^7$Li reactions), are more uncertain than currently believed. This is in agreement with the recent results of the NACRE compilation [24]. Here the authors recommend to fit the low-energy $^3\mathrm{H}(^4\mathrm{He},\gamma)^7\mathrm{Li}$ S-factor by the polynomial $S(E) = 0.1 - 0.15E + 0.13E^2$. This would imply $S^{-1}dS/dE\,(0) = -1.5$. This value is quite different from the one ($-2.056$) found in [7].

## 4 Conclusions

In summary, we have studied the $^3\mathrm{H}(^4\mathrm{He},\gamma)^7\mathrm{Li}$ and $^3\mathrm{He}(^4\mathrm{He},\gamma)^7\mathrm{Be}$ reactions in an extended two-cluster model that can take into account $^6\mathrm{Li}+p/n$ rearrangement channels. We have found that the inclusion of the $^6\mathrm{Li} + p/n$ channel significantly affects the reaction cross sections and some key properties of $^7$Be and $^7$Li. For the known correlations between the cross sections and, e.g., the quadrupole moments of $^7$Be and $^7$Li the results of the extended model (provided the $^6$Li binding energy is described sufficiently accurate) fit well into the trend, which is predicted by the simpler $\alpha + h/t$ description. We have pointed out that the value of $S_{34}(0)$, determined from the $S_{34}(0) - Q^{^7\mathrm{Li}}$ correlation in Ref. [7], seems now to be in conflict with the new accepted value of $^7$Li quadrupole moment. Finally we have discussed that the low-energy slope of the $^3\mathrm{He}(^4\mathrm{He},\gamma)^7\mathrm{Be}$ cross section, i.e. the value of $S'_{34}(0)$, might be more uncertain than currently believed.

Further studies in significantly larger model spaces (e.g., using a full seven-body dynamical description) will be interesting to see how well the present-day $\alpha + h/t$ cluster models reflect the true nature of the $^7$Be and $^7$Li nuclei.

*Acknowledgement.* We thank the Danish Research Council for financial support. The work of A. C. was supported by OTKA Grants F019701 and D32513, FKFP Grant 0242/2000, and by the Bolyai Fellowship of the Hungarian Academy of Sciences.

## References


1. J. N. Bahcall: *Neutrino Astrophysics.* Cambridge: Cambridge University Press 1989
2. R.F. Christy, I. Duck: Nucl. Phys. **24**, 89 (1961)
3. E. G. Adelberger et al.: Rev. Mod. Phys. **70**, 1265 (1998)
4. H. Walliser et al.: Phys. Rev. **C28**, 57 (1983); H. Walliser, H. Kanada, Y. C. Tang: Nucl. Phys. **A419**, 133 (1984)
5. K. Langanke: Nucl. Phys. **A457**, 351 (1986)
6. T. Mertelmeier, H. M. Hofmann: Nucl. Phys. **A459**, 387 (1986)
7. T. Kajino: Nucl. Phys. **A460**, 559 (1986)
8. T. Kajino, H. Toki, S. M. Austin: Astrophys. Journ. **319**, 531 (1987); **327**, 1060(E) (1988)
9. T. Altmeyer et al.: Z. Phys. **A330**, 277 (1988)
10. P. Mohr et al.: Phys. Rev. **C48**, 1420 (1993)
11. C. R. Brune, R. W. Kavanagh, C. Rolfs: Phys. Rev. **C50**, 2205 (1994)
12. A. Csótó, K. Langanke: Nucl. Phys. **A636**, 240 (1998)
13. M.. Kamimura: Prog. Theor. Phys. Suppl. **62**, 236 (1977)
14. H. R. Fiebig, A. Weiguny: Z. Phys. **A279**, 275 (1976)
15. P. Descouvemont, D. Baye: Nucl. Phys. **A407**, 77 (1983); Nucl. Phys. **A487**, 420 (1988)
16. D. R. Thompson, M. LeMere, Y. C. Tang: Nucl. Phys. **A268**, 53 (1977); I. Reichstein, Y. C. Tang: Nucl. Phys. **A158**, 529 (1970)
17. F. Tanabe, A. Tohsaki, R. Tamagaki: Prog. Theor. Phys. **53**, 677 (1975)
18. F. Ajzenberg-Selove: Nucl. Phys. **A490**, 1 (1988)
19. R. J. Spiger, T. A. Tombrello: Phys. Rev. **163**, 964 (1967)
20. H. Kräwinkel et al.: Z. Phys. **A304**, 307 (1982); P. D. Parker, R. W. Kavanagh: Phys. Rev. **131**, 2578 (1963); M. Hilgemeier et al.: Z. Phys. **A329**, 243 (1988); J. L. Osborne et al.: Phys. Rev. Lett **48**, 1664 (1982)
21. P. Pyykkö: Zeit. Naturforsch. **A47**, 189 (1992); H.-G. Völk, D. Fick: *Proceedings of the 7th International Conference on Polarization Phenomena in Nuclear Physics*, Paris (1990); M. Urban, A. J. Sadlej: Chem. Phys. Lett. **173**, 157 (1990)

22. F. Ajzenberg-Selove: Nucl. Phys. **A413**, 1 (1984)

23. B. K. Jennings, S. Karataglidis, T. D. Shoppa: Phys. Rev. **C58**, 3711 (1998)

24. C. Angulo et al. (NACRE Collaboration): Nucl. Phys. **A656**, 3 (1999)